Synchronization of multiple coupled rf-SQUID flux qubits

2009 New J. Phys. 11 123022

(http://iopscience.iop.org/1367-2630/11/12/123022)

New Journal of Physics
The open-access journal for physics

Synchronization of multiple coupled rf-SQUID flux qubits

R Harris[1,4], F Brito[1], A J Berkley[1], J Johansson[1], M W Johnson[1], T Lanting[1], P Bunyk[1], E Ladizinsky[1], B Bumble[2], A Fung[2], A Kaul[2], A Kleinsasser[2] and S Han[3]

[1] D-Wave Systems Inc., 100-4401 Still Creek Dr, Burnaby, BC V5C 6G9, Canada
[2] Jet Propulsion Laboratory, California Institute of Technology, Pasadena, CA, USA
[3] Department of Physics and Astronomy, University of Kansas, Lawrence, KS, USA
E-mail: rharris@dwavesys.com

New Journal of Physics **11** (2009) 123022 (10pp)
Received 21 July 2009
Published 21 December 2009
Online at http://www.njp.org/
doi:10.1088/1367-2630/11/12/123022

Abstract. A practical strategy for synchronizing the properties of compound Josephson junction (CJJ) radio frequency monitored superconducting quantum interference device (rf-SQUID) qubits on a multi-qubit chip has been demonstrated. The impact of small (∼1%) fabrication variations in qubit inductance and critical current can be minimized by the application of a custom-tuned flux offset to the CJJ structure of each qubit. This strategy allows for a simultaneous synchronization of the qubit persistent current and tunnel splitting over a range of external bias parameters that is relevant for the implementation of an adiabatic quantum processor.

Despite daunting obstacles, there is considerable interest in the development of solid state quantum information processors. This interest is fueled by the hope that breakthroughs in device fabrication will eventually facilitate the realization of large-scale quantum processors whose performance could surpass that of classical computers. Implementations based upon superconducting qubits have received particular attention ([1] and references therein). Considerable effort has been put into studying noise in such circuits [2, 3]. An equally pressing matter is fabrication variability, as qubits are acutely sensitive to variations in device

[4] Author to whom any correspondence should be addressed.

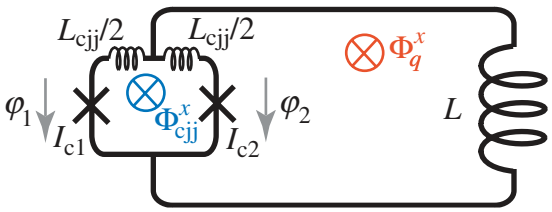

Figure 1. Schematic diagram of a CJJ rf-SQUID.

parameters [4, 5]. Current state of the art superconducting fabrication technology is limited, at best, to $\sim 1\%$ spreads in parameters such as Josephson junction critical currents and qubit inductances. The extent to which this variability affects the performance of a superconducting quantum computer is an important open problem. Therefore, it is relevant to demonstrate superconducting qubit designs and methods of operation that are insensitive to small variations in device parameters.

We wish to focus on a quantum Ising spin glass simulator [6, 7] constructed from superconducting flux qubits [8]. Such a device could be useful for solving optimization problems [9]. Each qubit i serves as a spin-1/2 subjected to transverse and longitudinal biases Δ_i and $\epsilon_i \equiv \mu_i B_i$, respectively. Here, μ_i represents the effective magnetic moment and B_i an externally controlled magnetic field. Pairwise couplings are realized by $J_{i,j} = M_{i,j}\mu_i\mu_j$, where $M_{i,j}$ is an externally controlled parameter. The system Hamiltonian at any time during operation has the form

$$\mathcal{H} = -\sum_{i=1}^{N} \frac{1}{2}\left[\epsilon_i \sigma_z^{(i)} + \Delta_i \sigma_x^{(i)}\right] + \sum_{i<j} J_{i,j}\sigma_z^{(i)}\sigma_z^{(j)}. \tag{1}$$

A particular adiabatic quantum algorithm, such as that described in [6], may require all μ_i and Δ_i to be nominally equivalent between qubits. While this choice of algorithm is by no means unique, it does represent the simplest implementation of an optimization procedure that utilizes quantum adiabatic evolution.

The objective of the work presented herein was to develop a practical strategy for minimizing the differences in qubit parameters between superconducting flux qubits due to fabrication variations. While typical device parameter variations from a reliable fabrication facility may only be of the order of 1%, it is argued that the resultant qubit properties, in particular Δ_i, can be exponentially sensitive to such variations. While no quantitative theory exists that dictates to what precision qubit properties must be identical in order to implement a given adiabatic quantum algorithm, it is clearly desirable to avoid situations in which Δ_i differ by orders of magnitude amongst a population of qubits. It is demonstrated herein that one can account for some fabrication variation when given a sufficiently forgiving qubit design that includes access to more than a single *in situ* tunable device bias.

One useful implementation of a superconducting flux qubit is the compound Josephson junction (CJJ) radio frequency monitored superconducting quantum interference device (rf-SQUID) [5], as depicted in figure 1. Here, a main loop of superconducting wire of inductance L_q is interrupted by a smaller loop of inductance L_{cjj} with two Josephson junctions of critical current I_{c1} and I_{c2}. The CJJ and main loop are subjected to external fluxes $\Phi_{cjj}^x = \Phi_0\varphi_{cjj}^x/2\pi$ and

$\Phi_q^x = \Phi_0\varphi_q^x/2\pi$, respectively, ($\Phi_0 \equiv h/2e$). The Hamiltonian for this system can be written as

$$\mathcal{H} = \sum_{i=1}^{2}\left[\frac{Q_i^2}{2C_i} - E_{Ji}\cos(\varphi_i)\right] + \sum_n U_n\frac{\left(\varphi_n - \varphi_n^x\right)^2}{2}, \tag{2}$$

where C_i and $E_{Ji} = I_{ci}\Phi_0/2\pi$ represent the capacitance and Josephson energy of junction i, respectively, and $[\Phi_0\varphi_i/2\pi, Q_j] = \mathrm{i}\hbar\delta_{ij}$. The inductive terms originate from the two closed loops with $n \in \{q, \mathrm{cjj}\}$, $L_q \equiv L + L_{\mathrm{cjj}}/4$ and $U_n \equiv (\Phi_0/2\pi)^2/L_n$. The qubit and CJJ loop phases are defined as $\varphi_q \equiv (\varphi_1 + \varphi_2)/2$ and $\varphi_{\mathrm{cjj}} \equiv \varphi_1 - \varphi_2$, respectively. This two-dimensional system can be reduced to an effective one-dimensional Hamiltonian if $L_q \gg L_{\mathrm{cjj}}$ because the plasma energy of the CJJ loop will be much higher than that of the main rf-SQUID loop. Setting $\varphi_{\mathrm{cjj}} = \varphi_{\mathrm{cjj}}^x$ and combining the Josephson terms,

$$\mathcal{H} \approx \frac{Q_q^2}{2C_p} + V(\varphi_q), \tag{3}$$

$$V(\varphi_q) = U_q\left\{\frac{\left(\varphi_q - \varphi_q^x\right)^2}{2} - \beta_{\mathrm{eff}}\cos\left(\varphi_q - \varphi_q^0\right)\right\}, \tag{4}$$

$$\beta_{\mathrm{eff}} = \beta_+\cos(\varphi_{\mathrm{cjj}}^x/2)\sqrt{1 + \left[\frac{\beta_-}{\beta_+}\tan(\varphi_{\mathrm{cjj}}^x/2)\right]^2}, \tag{5}$$

$$\varphi_q^0 \equiv 2\pi\frac{\Phi_q^0}{\Phi_0} = -\arctan\left(\frac{\beta_-}{\beta_+}\tan(\varphi_{\mathrm{cjj}}^x/2)\right), \tag{6}$$

where $C_p \equiv C_1 + C_2$, $[\Phi_0\varphi_q/2\pi, Q_q] = \mathrm{i}\hbar$ and $\beta_\pm \equiv 2\pi L_q(I_{c1} \pm I_{c2})/\Phi_0$. Focusing upon the two lowest lying states in the regime $\beta_{\mathrm{eff}} \lesssim -1$, one can recast equation (3) as a qubit Hamiltonian $\mathcal{H}_q = -\frac{1}{2}\left[\epsilon\sigma_z + \Delta\sigma_x\right]$, where $\epsilon = 2|I_q^p|(\Phi_q^x - \Phi_q^0)$. Note that by choosing $\beta_{\mathrm{eff}} < 0$, as achieved by operating the device with $-\Phi_0 < \Phi_{\mathrm{cjj}}^x < -\Phi_0/2$, the qubit degeneracy point $\epsilon \equiv 0$ is located at $\Phi_q^x = \Phi_q^0 \approx 0$ for $|\beta_-/\beta_+| \ll 1$. We have found this to be convenient in the laboratory as the more conventional choice of operating such a device with $0 < \Phi_{\mathrm{cjj}}^x < \Phi_0/2$ ($\beta_{\mathrm{eff}} > 0$) places the degeneracy point at $\Phi_q^x = \Phi_0/2 + \Phi_q^0$, which then necessitates applying large $\Phi_q^x \approx \Phi_0/2$ in order to operate it as a qubit. Denoting the ground and first excited state of equation (3) at the degeneracy point $\Phi_q^x = \Phi_q^0$ by $|+\rangle$ and $|-\rangle$, respectively, the spin states can be expressed as $|\uparrow\rangle = (|+\rangle + |-\rangle)/\sqrt{2}$ and $|\downarrow\rangle = (|+\rangle - |-\rangle)/\sqrt{2}$. The persistent current is then defined by $|I_q^p| \equiv |\langle\uparrow|(\Phi_q - \Phi_q^0)/L_q|\uparrow\rangle|$. The tunneling energy is given by $\Delta = \langle -|\mathcal{H}|-\rangle - \langle +|\mathcal{H}|+\rangle$. Both $|I_q^p|$ and Δ are functions of φ_{cjj}^x and therefore functions of the external bias Φ_{cjj}^x.

Equations (3)–(6) describe a system whose Hamiltonian is noticeably more complex than that in [5] purely due to what we refer to as junction asymmetry if $I_{c1} \neq I_{c2}$. In such a scenario, which is inevitable with any realistic fabrication process, $\beta_- \neq 0$ in equations (5) and (6), which leads to two important consequences. Firstly, the Φ_{cjj}^x-dependence of the tunnel barrier height $U_q\beta_{\mathrm{eff}}$ is modified compared to the ideal $\beta_- = 0$ case described in [5]. This impacts on the Φ_{cjj}^x-dependence of the qubit parameters $|I_q^p|$ and Δ. Secondly, junction asymmetry gives rise to an apparent Φ_{cjj}^x-dependent flux offset of the rf-SQUID, Φ_q^0, as given by equation (6). This effect, if not properly characterized and compensated for, can lead to a substantial unintended qubit

bias ϵ on the qubit if the intended mode of operation of the qubit involves modulating the tunnel barrier via $\Phi^x_{\rm cjj}$ [10].

The central focus of this paper is the description of a first step towards coming to terms with differences in the $\Phi^x_{\rm cjj}$ dependence of $|I^p_q|$ and Δ between CJJ rf-SQUID flux qubits on the same chip due to fabrication variations. By allowing for small independently tuned relative flux offsets in the CJJ bias $\delta\Phi_{\rm cjj}$ of each qubit, it is possible to simultaneously minimize differences in $|I^p_q|$ and Δ between qubits with slightly different L_q and $I_{\rm c} \equiv I_{\rm c1} + I_{\rm c2}$, thus *synchronizing* their properties. Consider $|I^p_q|$ and Δ in the regime $U_q\beta_{\rm eff} \gg \hbar\omega_p \equiv \hbar/\sqrt{L_qC_p}$. In this scenario, $|I^p_q|$ is primarily determined by the position of the minima of $V(\varphi_q)$ with only an extremely weak dependence upon C_p. In order to maintain constant $|I^p_q|$ in the presence of small variations in $\alpha \in \{L_q, I_{\rm c}\}$, the condition is $\beta_{\rm eff}(\alpha, \Phi^x_{\rm cjj}) = \beta_{\rm eff}(\alpha + \delta\alpha, \Phi^x_{\rm cjj} + \delta\Phi_{\rm cjj})$. To first order in $\delta\alpha/\alpha$, $\delta\Phi_{\rm cjj} \approx (\Phi_0/\pi)[\cot(\pi\Phi^x_{\rm cjj}/\Phi_0)]\delta\alpha/\alpha$. For $|\delta\alpha/\alpha| = 0.05$, one obtains $|\delta\Phi_{\rm cjj}| \sim 15\,{\rm m}\Phi_0$. Furthermore, one can use the Wentzel–Kramers–Brillouin (WKB) approximation [11] to write

$$\Delta \approx \frac{\hbar\omega_p}{\pi} {\rm e}^{-\frac{\Phi_0}{2\pi\hbar}\sqrt{2C_p}\int_{-a}^{a}{\rm d}\varphi_q\sqrt{V(\varphi_q)-\hbar\omega_p}}, \tag{7}$$

where $\pm a$ represent the classical turning points straddling the local maximum in $V(\varphi_q)$. The resultant form for Δ reveals that $\Delta(\alpha, \Phi^x_{\rm cjj}) = \Delta(\alpha + \delta\alpha, \Phi^x_{\rm cjj} + \delta\Phi_{\rm cjj})$, where $\delta\Phi_{\rm cjj} \approx \gamma(\Phi_0/\pi)[\cot(\pi\Phi^x_{\rm cjj}/\Phi_0)]\delta\alpha/\alpha$, with $\gamma \sim 1$ for $\alpha = L_q, I_{\rm c}$ and $\gamma \ll 1$ for $\alpha = C_p$. Interestingly, Δ shows a relatively weak dependence upon C_p as compared to L_q and $I_{\rm c}$. Thus perturbations of L_q and $I_{\rm c}$ ($\lesssim 5\%$) result in approximately the same shift of the CJJ bias dependence of both $|I^p_q|$ and Δ. In contrast, perturbations of C_p ($\lesssim 5\%$) have negligible impact upon $|I^p_q|$ but do influence the CJJ bias dependence of Δ.

The observations cited above indicate that one can compensate for small variations of L_q and $I_{\rm c}$ between CJJ rf-SQUID qubits by the application of custom-tuned CJJ bias offsets. For the average device parameters reported herein, Δ/h varies from $\sim 1\,{\rm MHz}$ to $\sim 10\,{\rm GHz}$ for $1 \lesssim |\beta_{\rm eff}| \lesssim 1.3$; since these qubits were designed with $\beta_+ \gtrsim 1.5$, the range of $\Phi^x_{\rm cjj}$ that was then relevant for operation of the qubits was $\lesssim 100\,{\rm m}\Phi_0$ wide. The strategy presented herein is to choose a unique reference CJJ bias $\Phi^0_{\rm cjj}$ for each qubit so that all $\Delta(\Phi^x_{\rm cjj} = \Phi^0_{\rm cjj})$ are equal. The expectation is that both $|I^p_q|(\Phi^x_{\rm cjj} - \Phi^0_{\rm cjj})$ and $\Delta(\Phi^x_{\rm cjj} - \Phi^0_{\rm cjj})$ will then be synchronized for all qubits within the range of $(\Phi^x_{\rm cjj} - \Phi^0_{\rm cjj})$ that is relevant for qubit operation.

In order to experimentally assess the CJJ synchronization strategy, we focused on a subset of CJJ rf-SQUID flux qubits embedded in a larger lattice of such devices (see figure 2). Each qubit is connected to three others via *in situ* tunable monostable CJJ rf-SQUID couplers, which we treat as classical mutual inductances [12]. We isolated a linear chain of six qubits by setting the intervening couplers to maximum antiferromagnetic coupling and the remaining unused couplers to provide zero coupling. Each qubit's state was probed via a dedicated hysteretic dc-SQUID sensor. The chip was fabricated from an oxidized Si wafer with Nb/Al/Al_2O_3/Nb trilayer junctions and three Nb wiring layers separated by sputtered SiO_2. It was mounted to the mixing chamber of a dilution refrigerator regulated at $T = 35\,{\rm mK}$ inside a PbSn superconducting magnetic shield surrounded by a μ-metal shield. The magnitude of the residual magnetic field in the vicinity of the chip after applying active magnetic field compensation above the critical temperature of the shield and subsequent cooling to $T = 35\,{\rm mK}$ was $\lesssim 9\,{\rm nT}$. External current biases were provided by a custom-built programmable room temperature 128-channel current

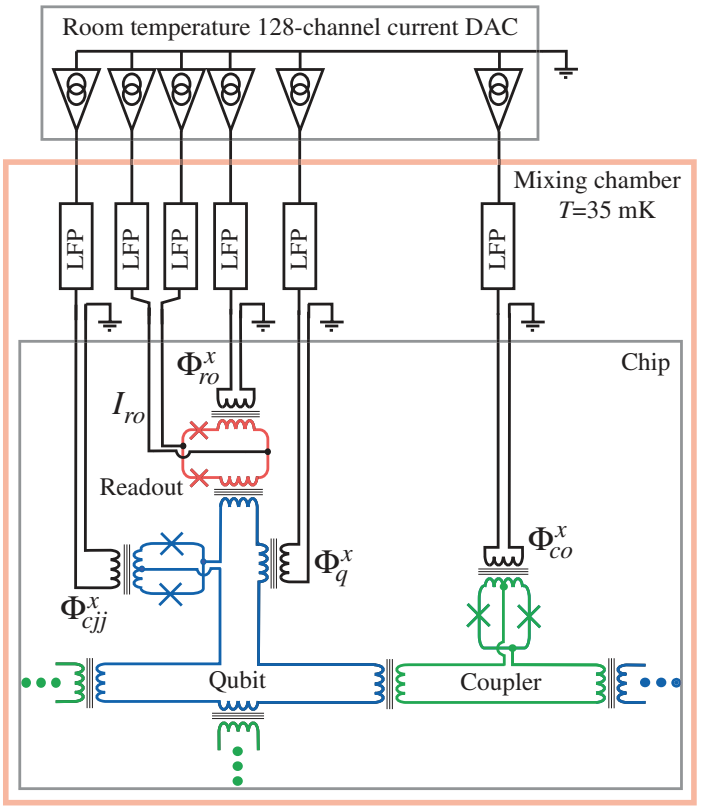

Figure 2. Schematic of a portion of a multi-qubit chip, bias line configuration and room temperature electronics. Ellipses indicate devices (alternating between qubit and coupler) that extend beyond the scope of the diagram.

digital-to-analog converter (DAC). Low pass filters (LPFs) with $f_c \approx 5\,\mathrm{MHz}$ were constructed from a combination of lumped element and copper powder filters secured to the mixing chamber. All mutual inductances and residual flux offsets were calibrated *in situ*. All relevant on-chip parasitic mutual inductances which led to unintended crosstalk were measured *in situ*. Crosstalk was compensated for for all applied current biases by multiplying a vector composed of a list of the desired flux biases by the inverted full inductance matrix for the device. However, it should be noted that the chip was designed with all sensitive devices residing close to a superconducting ground plane, which then reduced most on-chip parasitic mutual inductances to negligible levels.

To measure $|I_q^p|$ we employed hysteretic dc-SQUIDs as flux sensors. To begin, we initialized a given qubit, hereafter referred to as the source qubit, in the state $|\uparrow\rangle$, raised $U_q\beta_{\mathrm{eff}}$ to maximum height ($\Phi^x_{\mathrm{cjj}} = -\Phi_0$) and measured the change in flux sensed by its dc-SQUID. The process was repeated for the qubit initialized in the state $|\downarrow\rangle$ and the difference between the two measurements recorded. Knowing the readout-to-qubit mutual inductance $M_{\mathrm{ro-q}} = 6.46 \pm 0.17\,\mathrm{pH}$, obtained from an independent measurement, we determined $|I_q^p|_{\max} \equiv |I_q^p|(\Phi^x_{\mathrm{cjj}} = -\Phi_0)$ for each qubit. This measurement technique provided reliable results only if $M_{\mathrm{ro-q}}|I_q^p| > \delta\Phi_{\mathrm{ro}}$, where $\delta\Phi_{\mathrm{ro}} \sim 2\,\mathrm{m}\Phi_0$ represents a flux resolution limit imposed by the width of the dc-SQUID switching current distribution. In order to clearly resolve $|I_q^p|$ with $U_q\beta_{\mathrm{eff}}$ suppressed, we utilized a second qubit, hereafter referred to as the detector qubit, that was

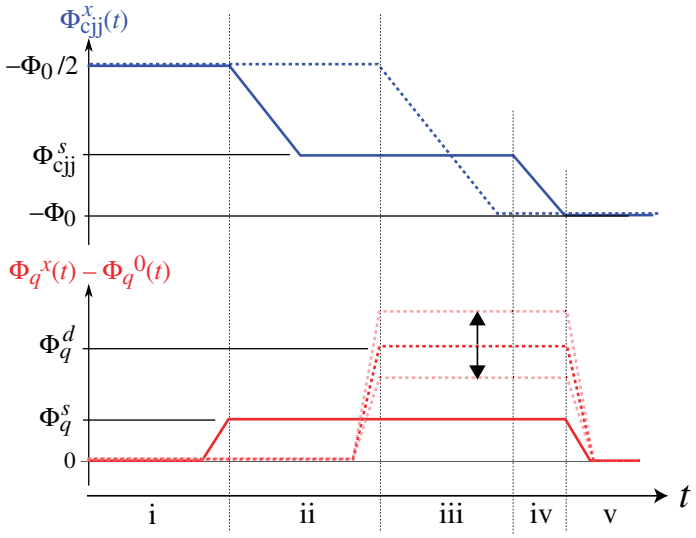

Figure 3. CJJ and flux bias waveforms versus time t for source (solid) and detector (dashed) qubits.

coupled to the source qubit via a coupler with effective mutual inductance $M_{\rm eff}$. Referring to figure 3, the sequence began with both qubit $V(\varphi_q)$ monostable ($\Phi^x_{\rm cjj} = -\Phi_0/2$ in equation (4)) and biased to their degeneracy points ($\Phi^x_q - \Phi^0_q = 0$) (i). Next, the source qubit was partially annealed to an intermediate CJJ bias $-\Phi_0 < \Phi^s_{\rm cjj} < -\Phi_0/2$ in the presence of a small bias $\Phi^s_q = \pm 2.1\,{\rm m}\Phi_0$ in order to initialize its state (ii). Thereafter, the detector qubit was fully annealed ($\Phi^x_{\rm cjj}$ ramped to $-\Phi_0$) in the presence of a variable bias Φ^d_q (iii). Finally, the source qubit was fully annealed (iv), both qubit flux biases were returned to their degeneracy point (v) and the state of the detector qubit was read (not shown). This annealing cycle was embedded inside a software feedback loop, which adjusted Φ^d_q until the particular bias for which the detector qubit could be found in $|\uparrow\rangle$ with probability $P_\uparrow = 1/2$ was found to within a specified precision. Performing the measurement for both signs of Φ^s_q and taking the difference between the two resultant values of Φ^d_q yielded $2M_{\rm eff}|I^p_q|$. Given $|I^p_q|_{\rm max}$ we then inferred $M_{\rm eff} = 1.35 \pm 0.04\,{\rm pH}$ for the five intervening couplers in the chain of six qubits. It was then possible to scale maps of $2M_{\rm eff}|I^p_q|$ versus $\Phi^x_{\rm cjj}$ to extract $|I^p_q|(\Phi^x_{\rm cjj})$.

To measure Δ of each qubit we used two methods. In the incoherent regime one can utilize macroscopic resonant tunneling (MRT) to trace out decay rate curves and extract Δ from fitting parameters [13]. The range of Δ that could be probed by this method had a practical upper bound because of the relatively low bandwidth of our bias lines. In the coherent regime, we employed a two-qubit procedure involving the waveform pattern shown in figure 3 in which Φ^s_q was scanned through the domain $[-3, +3]\,{\rm m}\Phi_0$ and Φ^d_q was again adjusted via a software feedback procedure to determine the shift in detector qubit degeneracy point at each Φ^s_q. Knowing $|I^p_q|(\Phi^x_{\rm cjj})$ allowed one to convert Φ^s_q and Φ^d_q into ϵ_1 and ϵ_2, respectively. For two coupled qubits in the limit $\Delta_2 \to 0$, the eigenenergies of equation (1) are given by $E_{1\pm} = \frac{1}{2}[\pm F(-) - \epsilon_2]$ and $E_{2\pm} = \frac{1}{2}[\pm F(+) + \epsilon_2]$, where $F(\pm) \equiv \sqrt{(\epsilon_1 \pm 2J_{1,2})^2 + \Delta_1^2}$. Using Boltzmann statistics, one can calculate the particular bias $\epsilon_2 = \epsilon_2^*$ for which the detector qubit will be found

with $P_{\uparrow} = 1/2$

$$\epsilon_2^* = \frac{F(+) - F(-)}{2} + k_B T \ln\left(\frac{1 + e^{-F(+)/k_B T}}{1 + e^{-F(-)/k_B T}}\right). \tag{8}$$

Note that in the limit $\Delta_1 \gg T, J_{1,2}$ equation (8) reduces to $\epsilon_2^* \approx J_{1,2}\epsilon_1/\sqrt{\epsilon_1^2 + \Delta_1^2} = J_{1,2} \langle g | \left| I_q^p \right| \sigma_z | g \rangle$, with $|g\rangle$ representing the ground state of the source qubit. Given independent calibrations of $|I_q^p|$ for both the qubits, M_{eff} and T, one can fit traces of ϵ_2^* versus ϵ_1 with equation (8) to extract Δ_1. This procedure is similar in spirit to that of [14]. In practice, the two-qubit method was found to be reliable only if $\Delta_1 > T$ and $M_{\text{eff}}|I_q^p| \gg \delta\Phi_n$, where $\delta\Phi_n$ represents the root mean squared low frequency flux noise experienced by the detector qubit. These constraints imposed lower and upper bounds, respectively, upon the range of Δ_1 that could be probed via this latter method.

Measurements of the CJJ bias dependence of $|I_q^p|$ and Δ are shown in figure 4. Here, we have plotted the data versus a relative CJJ bias where, for each qubit, a unique Φ_{cjj}^0 was chosen so that $\Delta(\Phi_{\text{cjj}}^0)/h = 20\,\text{MHz}$. The resultant values of Φ_{cjj}^0 are summarized in table 1. Recall that the central hypothesis of this paper is that the Φ_{cjj}^x dependence of the qubit parameters $|I_q^p|$ and Δ, as realized in CJJ rf-SQUIDs with slight variations in L_q and I_c, would be nearly identical provided one allows for a unique Φ_{cjj}^x offset for each qubit. We have subsumed this offset into the definition of the synchronization bias Φ_{cjj}^0. As a result of having chosen Φ_{cjj}^0 for each qubit so that all Δ are equal on one particular relative flux bias $\Phi_{\text{cjj}}^x - \Phi_{\text{cjj}}^0 = 0$, the six sets of $|I_q^p|$ data in figure 4(a) lie atop one another to within the measurement uncertainty over the range of $\Phi_{\text{cjj}}^x - \Phi_{\text{cjj}}^0$ for which Δ varies by five orders of magnitude. The Δ data in figure 4(b) show reasonable synchronization, albeit the results for q_2 show higher Δ in the coherent regime and slightly faster exponential decay as a function of Φ_{cjj}^x at small Δ. Otherwise, the values of Δ from the other five qubits are synchronized to within 20% over the range of $\Phi_{\text{cjj}}^x - \Phi_{\text{cjj}}^0$ shown. Note that if one had set Φ_{cjj}^0 equal for all qubits (no synchronization) that *none* of the Δ data in the regime where it varies exponentially with Φ_{cjj}^x would lie atop one another. In the worst case, the chosen Φ_{cjj}^0 for q_1 and q_2 differ by $15\,\text{m}\Phi_0$ in table 1. From figure 4(b), one can see that Δ changes by one decade for every $15\,\text{m}\Phi_0$ in Φ_{cjj}^x in the vicinity of the synchronization point $\Phi_{\text{cjj}}^x - \Phi_{\text{cjj}}^0 = 0$. As such, $\Delta(\Phi_{\text{cjj}}^x)$ for these two qubits differs by an order of magnitude in this regime. By choosing to plot the data as $\Delta(\Phi_{\text{cjj}}^x - \Phi_{\text{cjj}}^0)$ and operating the device in a manner that accounts for the relative CJJ offsets between qubits, one can avoid having to contend with such gross differences in qubit parameters. Finally, we note that the two-qubit method for extracting Δ proved particularly susceptible to corruption by low-frequency flux noise. For these qubits, drift measurements of the type reported in [3] revealed $1/f$ noise spectral densities with a mean amplitude $\sqrt{S_\Phi(1\,\text{Hz})} = 14 \pm 2\,\mu\Phi_0/\sqrt{\text{Hz}}$. Efforts to refine the two-qubit method and to reduce $1/f$ noise in our devices are ongoing.

In order to characterize the spread in CJJ rf-SQUID parameters, we have simultaneously fit $|I_q^p|$ and Δ for each individual qubit to the full CJJ rf-SQUID model equations (3)–(6) with $\beta_- \equiv 0$. The qubit parameters were obtained from this model by numerically solving for the two lowest lying eigenstates as a function of φ_q for a given Φ_{cjj}^x and $\Phi_q^x = 0$, thus yielding the states $|+\rangle$ and $|-\rangle$, and then calculating $|I_q^p|$ and Δ as described previously. We fit the model to the data from each qubit by substituting $\Phi_{\text{cjj}}^x \to \Phi_{\text{cjj}}^x - \Phi_{\text{cjj}}^0 + \bar{\Phi}_{\text{cjj}}^0$, where $\bar{\Phi}_{\text{cjj}}^0$ is defined as the mean value of Φ_{cjj}^0 reported in the bottom row of table 1, and then treating L_q, C_p and I_c

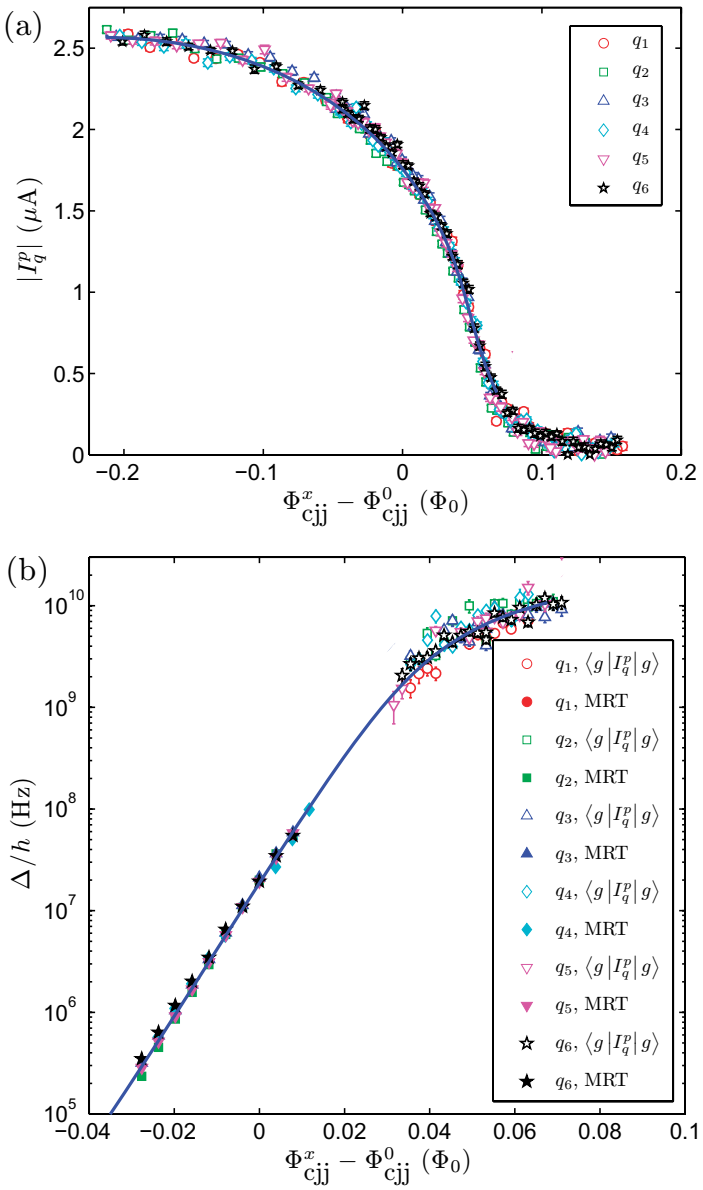

Figure 4. (a) $|I_q^p|$ and (b) Δ/h as a function of synchronized CJJ bias. Δ/h from the two-qubit and MRT measurement procedure are denoted as $\langle g|I_q^p|g\rangle$ and MRT in the legend, respectively. The solid curves are theoretical predictions using the mean device parameters quoted in table 1.

as free parameters. This method of fitting the data does not yield any information concerning junction asymmetry, but at least accounts for its effects by removing the relative CJJ offset $\Phi^0_{\rm cjj} - \bar{\Phi}^0_{\rm cjj}$ from the data. The best fit parameters for each qubit and their error estimates, as obtained from the nonlinear regression, are summarized in table 1. For comparison, we had estimated $L_q = 214\,\text{pH}$ and $C_p = 48\,\text{fF}$ from the design. To provide an independent estimate of I_c, we measured the maximum switching currents $I_{\rm sw}^{\rm max}$ of the dc-SQUID readouts, which contained two junctions of the same size as found in the qubits. These latter measurements

Table 1. Relative CJJ bias shifts $\Phi^0_{\rm cjj}$ and device parameters obtained by simultaneously fitting $|I^p_q|(\Phi^x_{\rm cjj})$ and $\Delta(\Phi^x_{\rm cjj})$.

Qubit	$\Phi^0_{\rm cjj}$ (mΦ_0)	L_q (pH)	C_p (fF)	$I_{\rm c}$ (μA)
1	-789 ± 5	200 ± 2	56 ± 1	2.58 ± 0.01
2	-774 ± 5	202 ± 2	56 ± 1	2.65 ± 0.01
3	-781 ± 5	200 ± 2	57 ± 1	2.63 ± 0.01
4	-784 ± 5	202 ± 2	55 ± 1	2.59 ± 0.01
5	-777 ± 5	200 ± 2	56 ± 1	2.65 ± 0.01
6	-785 ± 5	202 ± 2	54 ± 1	2.59 ± 0.01
Mean	-782 ± 12	201 ± 1	56 ± 1	2.62 ± 0.03

yielded a mean $I^{\rm max}_{\rm sw} = 2.30 \pm 0.05\,\mu$A. Modeling of the dc-SQUID switching process, given the designed inductance and capacitance of the dc-SQUIDs, revealed that the aforementioned value of $I^{\rm max}_{\rm sw}$ was consistent with $I_{\rm c} = 2.43 \pm 0.06\,\mu$A. At this point it is not clear why the critical currents of the dc-SQUID readouts were apparently systematically different than those of the rf-SQUID qubits. The quality of the fits to the qubit data shown in figure 4 proved most sensitive to $I_{\rm c}$ and relatively less sensitive to the choice of L_q and C_p. It is probable that fabrication variations between the Josephson junctions, roughly $\pm 1\%$ of the target $I_{\rm c}$, are the prime source of inter-qubit variability on this particular chip. To provide a succinct summary of the fitting results, the theoretical predictions for $\left|I^p_q\right|(\Phi^x_{\rm cjj} - \bar{\Phi}^0_{\rm cjj})$ and $\Delta(\Phi^x_{\rm cjj} - \bar{\Phi}^0_{\rm cjj})$, as obtained by using the mean CJJ rf-SQUID parameters listed at the bottom of table 1, are shown in figure 4.

One of the more challenging parameters to calibrate on this chip proved to be the nonlinear flux offset imparted by junction asymmetry Φ^0_q, as given by equation (6). We had observed a $\Phi^x_{\rm cjj}$-dependent shift of each qubit's degeneracy point in both the MRT and two-qubit Δ measurements discussed above. While not necessary for completing the device characterization reported upon herein, we managed to implement active compensation for this effect by *approximating* it as an effective linear crosstalk from the $\Phi^x_{\rm cjj}$ control line into Φ^x_q plus an additive constant over the operating range of $\Phi^x_{\rm cjj} - \Phi^0_{\rm cjj}$. This procedure was equivalent to expanding equation (6) to first order in $\Phi^x_{\rm cjj}$ about $\Phi^0_{\rm cjj}$. The fact that the sign and magnitude of the effective linear crosstalk varied between qubits with identical designs indicated that the effect was primarily due to junction asymmetry within each qubit, as opposed to a misidentified crosstalk.

Conclusions

A method for synchronizing the properties of multiple coupled CJJ rf-SQUID flux qubits with a small spread of device parameters due to fabrication variations was demonstrated. Both theory and experiment indicate that the application of a custom-tuned flux bias to each qubit CJJ loop is sufficient to compensate for $\pm 1\%$ differences in critical current. This strategy may prove to be an important step in the development of practical adiabatic quantum information processors.

Acknowledgments

We thank J Hilton, G Rose, P Spear, A Tcaciuc, F Cioata, E Chapple, C Rich, C Enderud, B Wilson, M Thom, S Uchaikin and M H S Amin. Samples were fabricated by the Microelectronics Laboratory of the Jet Propulsion Laboratory, operated by the California Institute of Technology under a contract with NASA. SH was supported in part by NSF grant no. DMR-0325551.

References

[1] Clarke J and Wilhelm F K 2008 *Nature* **453** 1031
[2] Simmonds R W *et al* 2004 *Phys. Rev. Lett.* **93** 077003
Martinis J M *et al* 2005 *Phys. Rev. Lett.* **95** 210503
Bialczak R C *et al* 2007 *Phys. Rev. Lett.* **99** 187006
Astafiev O, Pashkin Y A, Nakamura Y, Yamamoto T and Tsai J S 2004 *Phys. Rev. Lett.* **93** 267007
Schreier J A *et al* 2008 *Phys. Rev.* B **77** 180502
[3] Lanting T *et al* 2009 *Phys. Rev.* B **79** 060509
[4] Ramos R C *et al* 2001 *IEEE Trans. Appl. Supercond.* **11** 998
Koch J *et al* 2007 *Phys. Rev.* A **76** 042319
Mooij J E *et al* 1999 *Science* **13** 285
Paauw F G, Fedorov A, Harmans C J P M and Mooij J E 2009 *Phys. Rev. Lett.* **102** 090501
[5] Han S, Lapointe J and Lukens J E 1989 *Phys. Rev. Lett.* **63** 1712
Han S, Lapointe J and Lukens J E 1991 *Phys. Rev. Lett.* **66** 810
[6] Farhi E *et al* 2001 *Science* **292** 472
[7] Aharonov D, van Dam W, Kempe J, Landau Z and Lloyd S 2007 *SIAM J. Comput.* **37** 166
Biamonte J D and Love P J 2008 *Phys. Rev.* A **78** 012352
Zhang J *et al* 2009 *Phys. Rev.* A **79** 012305
[8] Kaminsky W M and Lloyd S 2003 *Quantum Computing and Quantum Bits in Mesoscopic Systems* MQC^2 (New York, NY: Kluwer)
[9] Boros E, Hammer P L and Tavares G 2007 *J. Heuristics* **13** 99
[10] Poletto S *et al* 2009 *New J. Phys.* **11** 013009
[11] Landau L D and Lifshitz E M 1977 *Quantum Mechanics* 3rd edn, vol 3 (Oxford: Butterworth-Heinemann) p 179
[12] Harris R *et al* 2009 *Phys. Rev.* B **80** 052506
[13] Amin M H S and Averin D V 2008 *Phys. Rev. Lett.* **100** 197001
Harris R *et al* 2008 *Phys. Rev. Lett.* **101** 117003
[14] Izmalkov A *et al* 2008 *Phys. Rev. Lett.* **101** 017003